Eco-evolutionary processes underlying early warning signals of population declines

Gaurav Baruah[1], Christopher F. Clements[1,2], Arpat Ozgul[1]

[1] Department of Evolutionary Biology and Environmental studies, University of Zurich

[2] School of Biosciences, University of Melbourne

Abstract

Environmental change can impact the stability of populations and can cause rapid declines in abundance. Abundance-based early warning signals have been proposed to predict such declines, but these have been shown to have limited success, leading to the development of warning signals based on the distribution of fitness-related traits such as body size. The dynamics of such traits in response to external environmental perturbations are controlled by a range of underlying factors such as reproductive rate, genetic variation, and plasticity. However, it remains unknown how such ecological and evolutionary factors affect the stability landscape of populations and the detectability of abundance and trait-based warning signals of population decline. Here, we apply a trait-based demographic approach and investigate both trait and population dynamics in response to gradual changes in the environment. We explore a range of ecological and evolutionary constraints under which the stability of a population may be affected. We show both analytically and with model-based simulations that strength of abundance-based early warning signals is significantly affected by ecological and evolutionary factors. Finally, we show that a unified approach, combining trait- and abundance-based information, significantly improves our ability to predict population declines.

1. Introduction

Predicting catastrophic and non-catastrophic collapses of populations and ecosystems in response to novel environmental pressures are critical if we are to mitigate the effects of global change and minimize the loss of biodiversity (Thomas *et al.*, 2004; Cardillo *et al.*, 2005). These collapses are however difficult to predict (Boettiger and Hastings, 2012; Clements *et al.*, 2015; Clements and Ozgul, 2018). One suite of methods, which may achieve this, are early warning signals derived from dynamic systems theory (van Nes and Scheffer, 2007; M. Scheffer *et al.*, 2009). Such methods assume that a dynamical system, for example a biological population, that is under increasing continuous external pressure, will show a property called critical slowing down (CSD) as it approaches a tipping point- the point at which the system's state can substantially change in response to a slight perturbation. Around the vicinity of this tipping point, the system takes longer to return to its original state after every perturbation (Wissel, 1984; Strogatz, 1994; Scheffer *et al.*, 2009).

The occurrence of CSD is a direct implication of the dominant eigenvalue of the system approaching zero (for continuous dynamical system) (van Nes and Scheffer, 2007) or 1 (for a discrete dynamical system) (Krko ek and Drake, 2014). As a direct consequence of CSD, statistical moments embedded within abundance time-series data, particularly variance and autocorrelation will show marked increase over time. These two indicators are the prominent abundance-based statistical metrics, and, along with various other metrics (Drake and Griffen, 2010; C. Boettiger and Hastings, 2012; Dakos *et al.*, 2012; Clements and Ozgul, 2016; Jarvis *et al.*, 2016; Clements and Ozgul, 2018; Dutta, Sharma and Abbott, 2018), are commonly known as early warning signals (EWS).

Changes in autocorrelation and variance are measures of the stability of a system, derived from the theory of alternative stable states (Wissel, 1984; Clements and Ozgul, 2018). Holling's (1973) fundamental work on stability and resilience laid the foundation for future work on deriving stability criteria for systems with alternative

equilibrium states. Stability of a dynamical system can be characterized by the classic ball-in-cup diagram (Holling, 1973; Nolting and Abbott, 2015; Clements and Ozgul, 2018), where the 'ball' represents the state of the system and the 'cup' represents the potential energy landscape (Fig.1). The stability of the system is thus quantified by the depth of the energy landscape, and resilience by the size of the cup (Dai, Korolev and Gore, 2015; Villa Martín *et al.*, 2015; Clements and Ozgul, 2018). In response to continuous exogenous pressure, the system loses resilience (for example, decline in population numbers) and the energy landscape shrinks (Fig. 1). Concurrent with the shrinkage of the landscape, there is also a decrease in the depth of the 'ball-in-cup' landscape signaling a loss in stability (Fig. 1). It is this loss in stability, which statistical EWSs such as variance and autocorrelation measure as an alternative for loss of global resilience of the system (Clements and Ozgul 2018). The shape of the ball-in-cup landscape thus determines the dynamics of the state variable in response to an exogenous environmental change (Beisner, Haydon and Cuddington, 2003).

However, the shape of the 'ball-in-cup' landscape can be changed not only by exogenous pressures, but can also be altered by intrinsic factors associated with the system's dynamics (Beisner, Haydon and Cuddington, 2003). Changes in these intrinsic factors might alter the location of an equilibrium state, or destabilize the current state, causing the system to arrive at a point closer to the other alternative state (Fig. 1). For a biological population, the state of the population will be characterized by its current abundance. Responses of this state variable (abundance) to an exogenous environmental pressure will be a combination of ecological and evolutionary responses controlled by factors such as genetic variation or plasticity (Price, Qvarnström and Irwin, 2003; Gienapp *et al.*, 2008; Ozgul *et al.*, 2010). For example, plastic responses to fluctuating changes in the exogenous environment are usually fast which consequently stabilizes population fluctuations (Reed *et al.*, 2010). However, if the environment keeps on changing, the population might not only deplete its plastic capacity but also its

standing genetic variation, which in turn leads to its eventual decline. Further, such a decline would also be conditional on the population's reproductive rate, with higher reproductive rate leading to a slower decline (Juan-Jordá *et al.*, 2015). In addition, due to continuous changes in the exogenous environment, selection pressures can subsequently increase leading to contemporary evolution (Yoshida *et al.*, 2003). Adaptive evolution would then depend on the amount of genetic variation present in the population with higher variation leading to faster evolution, which can either stabilize or destabilize population dynamics (Sanchez and Gore, 2013; Cortez, 2016). Since the dynamics of a population in response to an exogenous pressure is determined by the shape of its potential energy landscape (Beisner, Haydon and Cuddington, 2003), it is thus expected that these factors namely plasticity, genetic variation, and reproductive rate have the capacity to influence the shape of the ball-in-cup landscape. In turn, given that EWS are stability measures derived from alternative stable states theory (Beisner, Haydon and Cuddington, 2003; Scheffer *et al.*, 2009; Clements and Ozgul, 2018), it is very likely that strength in EWS and hence predictability of population decline might also be affected by these factors. Such theoretical expectations raise important practical questions: can predictability of population decline with the help of EWS be affected by such ecological and evolutionary factors?

Abundance-based measures of the stability of an ecological system might not be the only indicators of a population being forced by an external environment (Clements and Ozgul, 2016) . Phenotypic traits, such as body size, is one of the important traits that determines the fate of individuals as well as dynamics of population, and thus can provide crucial information regarding the current state of the population (Clements and Ozgul 2016b; Ozgul et al. 2014; Spanbauer et al. 2016). Recently, Clements & Ozgul (2016) showed, using data from experimental microcosms, that including body size information with EWS could significantly improve the predictive accuracy of population collapse. Such trait-based signals, have been further shown to be present in the historic

collapses of whale populations (Clements *et al.*, 2017). However, extensive research on the efficacy of such signals in comparison to abundance-based EWS is still in its infancy (Clements and Ozgul, 2018).

Here in this paper, we used a quantitative genetics framework to simulate the dynamics of a population in response to gradual environmental change. We track both the population dynamics and trait distribution until the simulated population collapses. We show that this particular model exhibits critical slowing down behavior and hence is expected to show EWS. We then assess whether genetic variation, plasticity in the trait, and net reproductive rate alter the ball-in-cup landscape (stability landscape) and consequently the strength in EWS. In addition, we assess the efficacy of trait-based EWS in comparison with abundance-based EWS and reiterate the ability of trait-based signals in accurately informing population collapses.

2. Materials and Methods

2.1 Mathematical model:

We model the joint dynamics of quantitative trait evolution and population size under density dependent regulation via the effects of selection (Gomulkiewicz and Holt, 1995; Chevin and Lande, 2010; Chevin, Lande and Mace, 2010) . We consider a population that has discrete generations where individuals have fitness that is determined by a single quantitative trait z under stabilizing selection with linear reaction norms (Gavrilets and Scheiner, 1993). Under these assumptions the dynamics of the population and the mean value of the trait can be written as (Lande, 2009) :

$$N_{t+1} = N_t \, \bar{R}_t \qquad (1)$$

$$\bar{z}_{t+1} = \bar{a}_t + \sigma_a^2 \frac{\partial ln\bar{W}}{\partial \bar{a}} + bu_t \qquad (2)$$

$\overline{R_t}$ is the average fitness of the population at generation *t*. $\bar{z}_{t+1}$ is the average value of the trait at generation *t+1*, $\bar{a}_t$ is the mean breeding value or genotypic value of the population at generation *t*, $\frac{\partial ln\overline{W}}{\partial \bar{a}}$ is the gradient of selection on the mean trait $\bar{z}$, σ_a^2 is the additive genetic variance, $\overline{W}$ is the mean fitness due to the trait z and bu_t quantifies the average plastic response of the trait at time t (see table 1).

Expanding $\overline{R_t}$ of equation (1) as follows:

$$\bar{R} = \int R(z)p(z)dz \qquad (3)$$

The integral in (3) over all trait values in the population gives the average fitness of the population. $R(z)$ in (3) is the absolute multiplicative fitness of an individual in the population with trait *z*. If *p(z)* is the distribution of the trait in the population and $R(z)$ defines the absolute fitness of an individual with trait z then, $R(z)$ can be further decomposed into :

$$R(z) = R_0^{(1-\frac{N}{K})} W(z) \qquad (4)$$

R_0 is the net reproductive rate which is under density dependent selection given by the exponent $\left(1-\frac{N}{K}\right)$ (Chevin and Lande, 2010). $W(z)$ is the gaussian stabilizing fitness function given as $W(z,\theta) = e^{-(z-\theta)^2/2w_z^2}$ with variance w_z^2 and optimum phenotype of θ. Individuals with trait values far from the optimum will have lower fitness compared to individuals whose trait value matches the optimum phenotype θ. Hence an individual's reproductive fitness $R(z)$ will not only dependent on the current density of the population but also by how far its trait value z is from the optimum phenotype θ (see Chevin and Lande, 2010).

Finally, the response of the primary phenotype z of an individual in this finite population to the external environment is modeled using linear reaction norms (Gavrilets and Scheiner, 1993; Lande and Shannon, 1996) :

$$z_{i,t} = a_{i,t} + bu_t + \epsilon \qquad (5)$$

where a is the breeding value of the individual i. The breeding value is normally distributed with mean $\overline{a}$ and additive genetic variance σ_a^2, and ϵ is the residual component with mean 0 and variance σ_ϵ^2. The slope b quantifies how plastic the trait z is in response to the environment. in our model b is constant meaning that plasticity in the trait cannot evolve (Chevin and Lande, 2010). We model an environment that determines the optimal phenotypic value θ_t for the primary phenotype z and also cues the plastic response. The optimal phenotype θ_t, is assumed to be linearly dependent on the external environment E that selects for a particular phenotypic value such that, $\theta_t = BE_t$.

We included stochasticity in the environment E_t as a Gaussian white noise process. The optimal phenotype θ_t, hence fluctuates as E_t fluctuates over a mean value over time t. As in Reed et al. (2010), the environmental cue u in equation (5) and the optimal phenotype θ are drawn from a bivariate normal distribution at each generation t. The covariance of u and θ in the bivariate normal distribution is given by $\sigma_{\theta,u} = \xi\sigma_\theta\sigma_u$ where ξ is the correlation between θ and the cue u. We assumed that variances in the cue σ_u and the optimum σ_θ are equal. This mimics the situation, for instance, when variation in food availability is correlated with inter annual variation in snow melt (Vuren and Armitage, 1991). ξ determines predictability of the environment such that ξ = 1 means the environmental cue is correlated with the optimum phenotype in a way that the plastic response tracks the optimum environment perfectly. In such a case, the strength in plastic response of the trait will be determined by b. If b is high there will be a strong plastic response and vice-versa. The optimal phenotype θ is drawn from the bivariate distribution at any generation t with mean value given by:

$$\theta_t = BE_t = \begin{cases} 0 & , t < t_{500} \\ B - B\frac{t}{500} & , t \geq t_{500} \end{cases} \qquad (6)$$

And the environmental cue u is drawn from the distribution with its mean value U_t over time given by:

$$U_t = \begin{cases} 0 & , t < t_{500} \\ 1 - c\frac{t}{500} & , t \geq t_{500} \end{cases} \quad (7)$$

With this, we can arrive at equation (2), which describes the changes in the mean phenotype $\bar{z}$ due to changes in the mean fitness $\overline{W}$ caused by the changes in the selecting environment E_t which dictates the dynamics of the optimum phenotype θ_t . The mean fitness $\overline{W}$ in equation (2) can be calculated as :

$$\overline{W} = \int W(z)p(z)dz = \sqrt{\frac{\sigma_w^2}{\sigma_z^2+\sigma_w^2}}\, e^{-(\overline{z_t}-\theta_t)^2/2(\sigma_w^2+\sigma_z^2)} .$$

The above model is based on the infinitesimal quantitative genetic model (Falconer and Mackay, 1996; Chevin and Lande, 2010).

2.2 Stability landscape and effective potential:

One approach to quantifying stability which is also fundamental to dynamical systems with alternative stable states is the 'ball-in-cup' analogy (Haydon, 2003; Villa Martín *et al.*, 2015). The different states of the dynamical system can be represented by a landscape and the state of the population at a particular moment by a ball in that landscape. The landscape of the dynamical system can be represented by an effective potential $V(n)$ (Beisner, Haydon and Cuddington, 2003; Villa Martín *et al.*, 2015). If a dynamical system (example a population) can be represented by a continuous differential equation in the form of: $\frac{dn}{dt} = g(n)$, then the effective potential of that dynamical system can be written as : $V(n) = -\int g(n)dn$ (Beisner, Haydon and Cuddington, 2003; Nolting and Abbott, 2015). For our dynamical system, $g(n) = \log\left(R_0^{\left(1-\frac{n}{k}+\beta-\gamma\right)}\right)$ (see supplementary 4). Here n is the state of the system, which in our

case is the log of the population size N. The effective potential of our dynamical system is then (supplementary 4):

$$V(n) = -\left(rn - \frac{\frac{r}{k}n^2}{2} + \beta rn - \gamma rn \right)$$

$$= \left(rn - \frac{\frac{r}{k}n^2}{2} + \frac{\log\left(\frac{\sqrt{(\sigma_w^2)}}{\sqrt{(\sigma_w^2 + \sigma_z^2}}\right)}{\log(R_0)} rn - \frac{(\bar{a} + bu_t - \theta_t)^2}{(R_0(\sigma_w^2 + \sigma_z^2))} rn \right) \qquad (9)$$

It is evident from the above equation (9) that the effective potential function is dependent on three parameters: r, β, γ, where $r = \log(R_0)$; $\beta = \frac{\log\left(\frac{\sqrt{(\sigma_w^2)}}{\sqrt{(\sigma_w^2+\sigma_z^2}}\right)}{\log(R_0)}$; $\gamma = \frac{(\bar{z}-\theta_t)^2}{(R_0(\sigma_w^2+\sigma_z^2))}$; $n = \log(N)$; $k = \log(K)$.

2.3 Equilibria and eigenvalues of the model:

The extinction equilibrium for the model is at $N^* = 0$ and the positive equilibrium for the model is at $N^* = K + \beta K - \gamma K$, where $\gamma = \frac{(\bar{z}-\theta_t)^2}{(R_0(\sigma_w^2+\sigma_z^2))}$; $\beta = \log\left(\frac{\sqrt{(\sigma_w^2)}}{\sqrt{(\sigma_w^2+\sigma_z^2}}\right) / \log(R_0)$ (see supplementary 1). Stability of the two equilibria are based on their corresponding eigenvalues, $\lambda = \frac{\partial}{\partial N} f(N)|_{N=N^*}$. Equilibria will be stable if magnitude of $\lambda < 1$ and unstable if magnitude of $\lambda > 1$ (Supplementary 1). Local stability analysis gives for the extinction equilibrium $N^* = 0$, $\lambda_1 = R_0^{1+\beta-\gamma}$ and for positive equilibrium $N^* = K + \beta K - \gamma K$, $\lambda_2 = 1 - (1 + \beta - \gamma) log R_0$. Thus, the extinction equilibrium $N^* = 0$, is always unstable since $\lambda_1 = R_0^{1+\beta-\gamma} > 1$ whenever $R_0 > 1$. On the other hand, the positive equilibrium $N^* = K + \beta K - \gamma K$ is stable conditional on the forcing parameter $\gamma = \frac{(\bar{z}-\theta_t)^2}{(R_0(\sigma_w^2+\sigma_z^2))}$ and $R_0 > 1$. Assuming that the phenotype is at its optimum ($\bar{z} = \theta$) i.e.,

$\gamma = 0$, then for $R_0 > 1$ the positive equilibrium is stable due to $\lambda_2 = 1 - (1 + \beta - \gamma) log R_0 < 1$. But as the forcing parameter $\gamma = \frac{(\bar{z} - \theta_t)^2}{(R_0(\sigma_w^2 + \sigma_z^2))}$ increases over time (due to θ_t shifting and the phenotype lagging behind), λ_2 slowly approaches 1 and the positive equilibrium which is $N^* = K + \beta K - \gamma K$ is initially stable but becomes unstable once λ_2 reaches 1. This happens when increases in the forcing parameter γ or increases in maladaptation causes average population growth rate $\bar{R}$ (4) also to reach 1. Once this happens, the extinction equilibrium then becomes stable at $\bar{R} = 1$ and the two equilibrium exchange stability at $\bar{R} = 1$. This is the definition of transcritical bifurcation. Moreover, as $\bar{R}$ approaches 1, the magnitude of λ_2 becomes larger and the recovery rate from external perturbation becomes slower (see supplementary 1 and 2). This indicates that there is CSD. λ_2 is directly related to return time, from which indicators like autocorrelation and standard deviation can be calculated (supplementary 2-3).

2.4 Simulations of population collapse

To complement our theoretical findings, we did simulations and forced the populations to collapse by increasing the rate of change in the environment E_t. We chose a rate of change in the environment θ_t in a way that populations collapsed regardless of any combination of parameter values. This was done by setting B =60 in (3) in all of our simulations. Environmental change was introduced at time point t = 500 (see equation 6 and 7), after populations have reached their carrying capacity. In all of our simulations, environmental predictability was high at $\xi = 1$, which means that the external environmental change and the environmental cue was highly correlated (see Reed et al. 2010). For each parameter value of a factor (genetic variation, plasticity, net reproductive rate) we did 100 independent simulations of population collapse. For each population time series, we first estimated the bifurcation time-point by fitting

generalized additive models (GAMs) to $\frac{N_{t+1}}{N_t}$ over time *t*. The bifurcation time point was recorded as the first point at which $\frac{N_{t+1}}{N_t}$ dropped and stayed below 1.

2.4.1 Abundance-based EWS

For abundance-based EWS analyses, the length of the time-series used was of the same length for each factor (genetic variation, plasticity, net reproductive rate) in question. For each parameter value of each factor in question, we used time-series data to the estimated bifurcation point. We discarded time-series data after the bifurcation point. The bifurcation time point however varied from t = 510 to t =545 time point, due to different factors in question. Note that the optimum environment shifted at t=500 time point. Although the bifurcation time point was within the range of 510 to 545 time point, population extinction however always occurred after t=590, regardless of the factor in question (see timeseries data, Fig. S3-S5). Next, we analyzed 50 abundance data points before each of the bifurcation time points. This ensured normalization of the length of each time series and minimized the effect of varying length of timeseries.

We then applied generic EWS of population collapse by using the *earlywarnings* package in R. We focused our analysis on two specific indicators namely autocorrelation at the first-lag (AR1) and standard deviation (SD) as most of the other indicators – such as first-order autoregressive coefficient or coefficient of variation – could be theoretically derived from these parameters (Dakos et al. 2012). The two indicators AR1 and SD were calculated using a predefined sliding window which was 50% of the abundance time-series being analyzed. We z-standardized the leading indicators so that it would be easier to incorporate information from phenotypic trait later in our analyses. We used Gaussian detrending to remove any trend in the abundance time-series and used Kendall's Tau correlation coefficient of the indicators prior to the estimated bifurcation point as an indicator of an approaching collapse. Kendall's tau is a non-parametric measure of rank correlation used to identify an increasing trend. Kendall's tau takes

values in the range of [-1,1]. Strong positive Kendall's Tau correlations of the statistical indicators (SD and AR1) with time would indicate an approaching population collapse (Dakos et al. 2012). If Kendall's tau correlation coefficient for an EWS was less than 0.4, we considered that EWS as a false negative. Hence, we quantified reliability of EWS as the rate of false negatives: the number of times in replicate simulations the Kendall's tau correlation coefficient was less than 0.40 (for results of false negatives for lower cut-off of 0.20 and for higher cut-off of 0.60, see supplementary Fig. S10-S11). Higher proportion of false negatives would indicate less reliability of EWS and vice-versa.

2.4.2 Trait-based EWS

To evaluate the efficacy of trait-based EWS (Clements and Ozgul, 2016), information from mean phenotype $\bar{z}$ was incorporated with the leading indicators in an additive manner. To include information from average phenotypic value, we first z-standardized the trait time-series. The length of the phenotypic time-series that was used was the same as the corresponding abundance time-series. Before a population decline, SD and AR1 are expected to increase over time, while the trait is expected to decline. Consequently, the z-standardized values of phenotypic timeseries were multiplied by -1 so that they could be included with the other two standardized statistical metrics such as SD and AR1. The values of standardized EWS such as SD and AR1 were added additively with standardized mean phenotypic time series to quantitatively create trait-based signals. We evaluated three trait-based EWS metrics namely *AR1+trait, AR1+SD+trait, SD+trait* and compared how the metrics that included information from the mean phenotype improved predictability of population collapse when compared with the abundance-based EWS like *AR1, SD.* We quantified Kendall's Tau correlation coefficient as an indicator for strength of predictability of population collapse and reliability of the trait-based EWS as the rate of false negatives.

2.4.3 Adaptive plasticity: To assess the role of adaptive plasticity *b*, we simulated 100 replicate population collapses for each parameter value of *b,* which ranged from low to high: 0.05, 0.1, 0.2, 0.3, 0.4, and 0.5. While we varied plasticity, we fixed $\sigma_a^2 = 0.2$, and R_0 at 1.2. The width of the fitness function determines the strength of selection in the trait. We fixed the width of the fitness function at $\sigma_w^2 = 25$, which would indicate medium strength in selection. Usually, $\sigma_w^2 = 50$ would indicate weak strength in selection and $\sigma_w^2 = 5$ would indicate strong selection (Chevin and Lande 2010).

2.4.4 Genetic variation: The levels of genetic variation σ_a^2 used for the simulations of population collapse are 0.05, 0.1, 0.2, 0.3, 0.4,0.5. Adaptive plasticity *b*, net reproductive rate R_0 and σ_w^2 were kept at 0.2, 1.2 and 25 respectively.

We also did simulations where we relaxed the assumption of genetic variation (σ_a^2) remaining constant during population collapses. For details see supplementary 5.

2.4.5 Net reproductive rate: To assess the role R_0, we simulated 100 replicate population collapses. The levels of R_0 used for the simulations of population collapse were 1.1, 1.2, 1.3, 1.4, and 1.5. Adaptive plasticity *b*, genetic variation σ_a^2 and σ_w^2, were kept at 0.2, 0.2 and 25 respectively.

3. Results

3.1 Effective potential

3.1.1 Strength in plasticity

The term $\gamma = \frac{(\bar{z}-\theta_t)^2}{(R_0(\sigma_w^2+\sigma_z^2))}$ in equation (9) is the evolutionary lag due to maladaptation of the mean phenotype with the optimum (Lande, 2009). The effective potential becomes narrower with increasing strength in plasticity and consequentially increases stability, i.e., the potential function becomes more negative (Fig. 2). Since return time and stability are inversely related (Dai, Korolev and Gore, 2015), return time decreases with

increasing strength in plasticity (Supplementary 2, Fig. S1). In other words, the population quickly recovers with every perturbation if strength in plasticity is high.

3.1.2 Genetic variation

The mean phenotype has variance of $\sigma_z^2 = \sigma_a^2 + \sigma_\epsilon$. Assuming residual component σ_ϵ to be zero, phenotypic variance is then equal to additive genetic variance, $\sigma_z^2 = \sigma_a^2$. Inspection of the equation (9) reveals that high additive genetic variance causes the effective potential to be more positive when compared with low σ_a^2 and consequently decreases stability, i.e., the effective potential becomes less negative (Fig. 2; the more negative the effective potential, more stable the population is). Reduction of stability and effective potential energy is higher for populations with low genetic variance whenever they are forced to collapse compared to populations with high genetic variance (Fig. 2). Further, return time also increases with increasing additive genetic variance (supplementary 2, Fig. S1).

3.1.3 Net reproductive rate

From equation (9), we also see that higher values of R_0 lead to higher stability and narrow potential curve for a given state of the population (Fig. 2). Loss in stability is more when R_0 is higher for the same rate of change in the environmental change when compared with a lower R_0. Further, return time also decreases with increasing R_0 (supplementary 2, Fig. S1).

3.2 Simulations of population collapse: abundance-based EWS

3.2.1 Strength in plasticity

The strength of EWSs of population collapse (Kendall's Tau value) was much higher in populations which had high adaptive plasticity $\boldsymbol{b}$ = 0.6 (Fig. 3a, b) when compared with populations with low adaptive plasticity. Moreover, the rate of false negatives decreased for SD as strength in plasticity increased (Fig. 5a). Rate of false negatives however remained more or less same for AR1 across different plasticity levels (Fig. 5a).

371 *3.2.2 Genetic variation*

372 Higher genetic variation in the population led to slight decrease in detectability of
373 population decline than in populations with lower genetic variation, particularly for SD
374 (Fig. 3c, d). Moreover, the rate of false negatives for SD decreased slightly as genetic
375 variation decreased (Fig. 5b). For AR1 the rate of false negatives remained more or less
376 the same (Fig. 5b).

377 *3.2.3 Net reproductive rate*

378 Strength in EWS was lower in populations with lower R_0 when compared with higher R_0
379 , particularly for SD (Fig. 3e). AR1 however showed a slightly different result (Fig. 3f). In
380 case of reliability of abundance-based EWS, the rate of false negatives decreased for SD
381 as net reproductive rate increased (Fig. 5c). However, for AR1 rate of false negatives
382 increased as R_0 increased (Fig. 5c).

383 *3.3 Simulations of population collapse: trait-based EWS*

384 Trait-based EWS improved the strength of EWS of population collapse (Fig. 4, Fig S8-
385 S9). In principle, *AR1* was the least efficient of all the signals compared. However, when
386 trait information was included with *AR1*, strength in trait-based *AR1 (trait+AR1)*
387 improved significantly (Fig.4, Fig. 5). Overall, the Kendall's Tau value of SD and *SD+trait*
388 was relatively higher than all the other trait-based and abundance-based EWS. This was
389 consistent across all the factors analyzed such as genetic variation, plasticity (Fig.4, Fig.
390 S8-S9). The rate of false negatives for net reproductive rate decreased from around 0.25
391 to 0 for *trait+SD* as net reproductive rate increased (Fig. 5c). The rate of false negatives
392 was highest for AR1 across all factors analyzed (Fig. 5a-c). For plasticity, the rate of false
393 negatives decreased as strength in plasticity increased, but this was however opposite
394 for genetic variation where the false negatives slightly increased as genetic variance
395 increased (Fig. 5b). Furthermore, even though AR1 had the highest number of false
396 negatives, false negatives of *AR1+trait* significantly decreased (Fig. 5).

4. Discussion

The early detection of population collapse with the help of EWS provides a unique tool to highlight conservation efforts to a population approaching an impending transition. These tools are relatively simple, easy to use, as they only require state-based data like abundance and hence are applicable to a variety of ecological systems. However, we show here that factors intrinsic to a population in question such as genetic variation, plasticity or net reproductive rate could significantly alter stability of a population as well as strength and reliability in EWS of population decline.

The detectability of EWSs is dependent not only on the relation between stability and resilience but is also determined by a variety of factors including sampling frequency, and the strength and type of external forcing (Dai, Korolev, and Gore 2015; Clements et al. 2015a; Clements and Ozgul 2016). Here we add to this body of knowledge by demonstrating that the stability of a system can also be altered by intrinsic factors such as genetic variation, plasticity and net reproductive rate. These changes to the effective potential in turn led to stronger EWS being observed, whenever changes in the external optimum caused a population to lose a significant amount of potential energy (Fig. 1). In other words, stronger EWSs would be observed whenever a population is forced to move from a deeper point in the potential energy curve (more stable) to its tipping point compared to another population, which is lying on a shallower potential (less stable) (Fig. 2). Our findings also suggested that the utility of EWS was strongly determined by factors that are intrinsic to a population such as genetic variation, net reproductive rate and plasticity.

Higher strength in plasticity in the phenotype significantly affected the detectability of population collapse (Fig. 2). Strength in plasticity altered the response and the dynamics of a population to changes in the external environment. When plasticity was high the response of the phenotype tracked the environment perfectly causing the population to

423 stabilize in response to fluctuating changes in the environment (Fig. S3) (Charmantier *et*
424 *al.*, 2008; Reed, Schindler and Waples, 2011). The stability of a population is also
425 reflected in short return time to equilibrium (van Nes and Scheffer, 2007). This was true
426 for the case where the strength in plasticity was high (Fig. S1). Moreover, the basin of
427 attraction for a highly plastic population was deeper when compared to a less plastic
428 population, which was shallower. To push a highly plastic population from the deepest
429 point in its basin of attraction to the tipping point, the energy loss would be more,
430 compared to a less plastic population which was lying in a much shallower basin. The
431 loss in energy from driving the highly plastic population from the deepest point to its
432 tipping point was reflected in stronger EWS when one compared it with another less
433 plastic population. Consequently, for the same rate of change in the environment, higher
434 values of plasticity lead to stronger and more reliable EWS of population collapse.

435 Similarly, the effective potential of our dynamical system was also altered by genetic
436 variation (Fig. 2), with higher genetic variation leading to a shallower stability landscape
437 than that of a population with lower genetic variation. High additive genetic variance
438 created what was called a 'genetic load' that lowered the overall population growth rate
439 (Lande 1976; Lande and Shannon 1996; Chevin, Lande, and Mace 2010). This was due to
440 stabilizing selection acting on the mean phenotype. Due to this genetic load caused by
441 high additive genetic variance, population growth rate at equilibrium was lower causing
442 the effective potential to be closer towards the tipping point compared to another
443 population having a lower genetic variation. Hence for the same rate of external
444 environmental change, the loss of potential energy was different when one compared a
445 population with high genetic variation to that with low genetic variation. As a result, the
446 performance of EWS was affected with slightly lower detectability and lower reliability
447 of population collapse when there was higher genetic variation (Fig. 3, Fig. 5b). This
448 result however did not mean that genetic variation was detrimental for long-term
449 population persistence. Time to extinction was however longer for populations with

450 higher genetic variation when compared with a population which had a lower genetic
451 variation in the trait (Fig S2)(Yvonne and Hoffmann, 2009; Robinson, Wares and Drake,
452 2013). High genetic variation is necessary for rapid adaptation via genetic evolution,
453 which then aids in evolutionary rescue (Ashander, Chevin and Baskett, 2016).
454 However, our model simulations and analyses of EWS were mainly focused on short
455 transient dynamics after the start of the external optimum change. Further, due to
456 continuous and fast rate of environmental deterioration, adaptation or evolutionary
457 rescue by genetic evolution (Lande 2009; Chevin and Lande 2010) was not possible in
458 our model and the populations eventually collapsed.

459 Decreasing population size in response to environmental deterioration and directional
460 selection acting towards a mean phenotype could both lead to depletion of additive
461 genetic variance (Barton and Keightley, 2002). We took this account in our simulations
462 by following a framework developed in (Bürger, 2000). Using this framework, we find
463 that depletion of genetic variation over time did not affect the strength of EWS
464 compared with when genetic variation remained constant (See Fig S6).

465 Net reproductive rate also had a significant effect on the stability of populations,
466 detectability and reliability of EWS of population collapse. Populations with a lower net
467 reproductive rate declined steeply and earlier than populations with higher net
468 reproductive rate for the same rate of external environmental change (Fig. S5). Higher
469 net reproductive rate buffered the population from declining immediately after the
470 environment shifted when compared to a population with lower reproductive rate
471 (Juan-Jordá *et al.*, 2015). Consequently, for the same rate of change in the external
472 optimum environment, populations with lower reproductive rate recovered slowly due
473 to a wide basin of attraction than populations with higher net reproductive rate (Fig. 2,
474 Fig. S1) and hence strength in EWS was more pronounced in the latter.

475 Our modeling results suggested that including fitness-related trait information could
476 significantly improve the strength and reliability in EWS of population collapse. SD and
477 trait-based EWS (*SD+trait*) produced strongest and reliable signals. Inclusion of
478 phenotypic trait information alongside the leading indicators produced less distributed,
479 consistent and stronger Kendall's tau values compared to the generic abundance-based
480 EWS (Fig. 4, Fig S8-S9). In all the different biological factors examined in our study SD
481 and *SD+trait* metric performed the best overall. In response to a directional change in
482 the external optimum environment, shift in the mean phenotypic trait occurred over
483 time even if there were no significant increases in either AR1 or SD. Furthermore,
484 including information from the mean phenotype alongside EWS statistics would depend
485 not only on whether the mean phenotype responded to the external forcing but also on
486 the nature of the external environmental forcing itself (Clements and Ozgul, 2016). Body
487 size is suggested to be an ideal candidate to be included with the leading indicators
488 (Clements and Ozgul, 2016). Shifts in body size have previously been shown to occur
489 before population collapse in whales, with true positive EWS being detectable earlier
490 when information from the body size was included in the EWS (Clements *et al.*, 2017).

491 In conclusion, we showed that predictability of population collapse was affected by
492 factors intrinsic to a population like genetic variation, strength in adaptive plasticity and
493 net reproductive rate. Changes in these factors can not only alter the underlying
494 phenotypic and population dynamics, but also the potential energy landscape.
495 Consequently, due to the alteration of the potential energy landscape, the detectability
496 of EWS was severely hampered. However, if information from fitness-related trait was
497 incorporated with EWS, the strength in predicting population collapses increased
498 significantly. Our results add to the body of evidence suggesting that the inclusion of
499 trait dynamic information alongside the generic EWS should provide more accurate
500 forecasts of the future state of biological systems.

Author's Contribution:

REFERENCES

Ashander, J., Chevin, L.-M. and Baskett, M. L. (2016) 'Predicting evolutionary rescue via evolving plasticity in stochastic environments', *Proceedings of the Royal Society B: Biological Sciences*. doi: 10.1098/rspb.2016.1690.

Barton, N. H. and Keightley, P. D. (2002) 'Understanding quantitative genetic variation.', *Nature reviews. Genetics*, 3(1), pp. 11–21. doi: 10.1038/nrg700.

Beisner, B., Haydon, D. and Cuddington, K. (2003) 'Alternative stable states in ecology', *Frontiers in Ecology and the Environment*. Wiley-Blackwell, 1(7), pp. 376–382. doi: 10.1890/1540-9295(2003)001[0376:ASSIE]2.0.CO;2.

Boettiger, C. and Hastings, A. (2012) 'Quantifying limits to detection of early warning for critical transitions.', *Journal of the Royal Society, Interface / the Royal Society*. doi: 10.1098/rsif.2012.0125.

Boettiger and Hastings (2012) 'Quantifying limits to detection of early warning for critical transitions', *Journal of The Royal Society Interface*, pp. 2527–2539. doi: 10.1098/rsif.2012.0125.

Bürger, R. (Reinhard) (2000) *The mathematical theory of selection, recombination, and mutation*. Wiley.

Cardillo, M. *et al.* (2005) 'Multiple causes of high extinction risk in large mammal

species.', *Science (New York, N.Y.)*, 309(5738), pp. 1239–41. doi: 10.1126/science.1116030.

Charmantier, A. *et al.* (2008) 'Adaptive phenotypic plasticity in response to climate change in a wild bird population.', *Science (New York, N.Y.)*, 320(5877), pp. 800–803. doi: 10.1126/science.1157174.

Chevin, L. M., Lande, R. and Mace, G. M. (2010) 'Adaptation, plasticity and extintion in a changing enviroment: towards a predictive theory', *PLoS biology*. Edited by J. G. Kingsolver. Public Library of Science, 8(4), pp. 1–8.

Chevin and Lande (2010) 'When do adaptive plasticity and genetic evolution prevent extinction of a density-regulated population?', *Evolution*, 64(4), pp. 1143–1150. doi: 10.1111/j.1558-5646.2009.00875.x.

Clements *et al.* (2015) 'Factors Influencing the Detectability of Early Warning Signals of Population Collapse', *The American Naturalist*, 186(1), pp. 50–58. doi: 10.1086/681573.

Clements *et al.* (2017) 'Body size shifts and early warning signals precede the historic collapse of whale stocks', *Nature Ecology & Evolution*. doi: 10.1038/s41559-017-0188.

Clements, C. F. and Ozgul, A. (2016) 'Rate of forcing and the forecastability of critical transitions', *Ecology and Evolution*, In press(April), pp. 7787–7793. doi: 10.1002/ece3.2531.

Clements and Ozgul, A. (2016) 'Including trait-based early warning signals helps predict population collapse', *Nature Communications*, 7, p. 10984. Available at: http://www.nature.com/doifinder/10.1038/ncomms10984.

Clements and Ozgul, A. (2018) 'Indicators of transitions in biological systems', *Ecology Letters*. Edited by J. Metcalf. Wiley/Blackwell (10.1111). doi: 10.1111/ele.12948.

Cortez, M. H. (2016) 'How the Magnitude of Prey Genetic Variation Alters Predator-Prey Eco-Evolutionary Dynamics.', *The American naturalist*. University of Chicago PressChicago, IL, 188(3), pp. 329–41. doi: 10.1086/687393.

Dai, L., Korolev, K. S. and Gore, J. (2015) 'Relation between stability and resilience determines the performance of early warning signals under different environmental drivers.', *Proceedings of the National Academy of Sciences of the United States of America*. National Academy of Sciences, 112(32), pp. 10056–61. doi: 10.1073/pnas.1418415112.

Dakos, V. *et al.* (2008) 'Slowing down as an early warning signal for abrupt climate change.', *Proceedings of the National Academy of Sciences of the United States of America*, 105(38), pp. 14308–12. doi: 10.1073/pnas.0802430105.

Dakos, V. *et al.* (2012) 'Methods for detecting early warnings of critical transitions in time series illustrated using simulated ecological data', *PLoS ONE*, 7(7). doi: 10.1371/journal.pone.0041010.

Drake, J. M. and Griffen, B. D. (2010) 'Early warning signals of extinction in deteriorating environments.', *Nature*. Nature Publishing Group, a division of Macmillan Publishers Limited. All Rights Reserved., 467(7314), pp. 456–9. doi: 10.1038/nature09389.

Dutta, P. S., Sharma, Y. and Abbott, K. C. (2018) 'Robustness of early warning signals for catastrophic and non-catastrophic transitions', *Oikos*. Wiley/Blackwell (10.1111). doi: 10.1111/oik.05172.

Falconer, D. S. and Mackay, T. F. C. (1996) *Introduction to Quantitative Genetics (4th Edition)*, *Trends in Genetics*. Available at: http://www.amazon.com/Introduction-Quantitative-Genetics-Douglas-Falconer/dp/0582243025.

Gavrilets, S. and Scheiner, S. M. (1993) 'The genetics of phenotypic of reaction norm shape V . Evolution', *Journal of Evolutionary Biology*, 6(1), pp. 31–48. doi:

10.1046/j.1420-9101.1993.6010031.x.

Gienapp, P. *et al.* (2008) 'Climate change and evolution: Disentangling environmental and genetic responses', *Molecular Ecology*, pp. 167–178.

Gomulkiewicz, R. and Holt, R. D. (1995) 'When does evolution by natural selection prevent extinction?', *Evolution*, 49(1), pp. 201–207. Available at: http://www.jstor.org/stable/10.2307/2410305%5Cnpapers2://publication/uuid/AF75FB13-CA45-471F-9595-604002DDAB20.

Haydon, D. (2003) 'Alternative stable states in ecology', *Frontiers in Ecology*. doi: 10.1890/1540-9295(2003)001[0376:ASSIE]2.0.CO;2.

Holling, C. S. (1973) 'Resilience and Stability of Ecological Systems', *Annual Review of Ecology and Systematics*. Annual Reviews 4139 El Camino Way, P.O. Box 10139, Palo Alto, CA 94303-0139, USA , 4(1), pp. 1–23. doi: 10.1146/annurev.es.04.110173.000245.

Jarvis, L. *et al.* (2016) 'Early warning signals detect critical impacts of experimental warming', *Ecology and Evolution*. doi: 10.1002/ece3.2339.

Juan-Jordá, M. J. *et al.* (2015) 'Population declines of tuna and relatives depend on their speed of life', *Proceedings of the Royal Society B: Biological Sciences*, 282(1811), p. 20150322. doi: 10.1098/rspb.2015.0322.

Krko ek, M. and Drake, J. M. (2014) 'On signals of phase transitions in salmon population dynamics', *Proceedings of the Royal Society B: Biological Sciences*, 281(1784), pp. 20133221–20133221. doi: 10.1098/rspb.2013.3221.

Lande (2009) 'Adaptation to an extraordinary environment by evolution of phenotypic plasticity and genetic assimilation', *Journal of Evolutionary Biology*, 22(7), pp. 1435–1446. doi: 10.1111/j.1420-9101.2009.01754.x.

Lande, R. (1976) 'NATURAL SELECTION AND RANDOM GENETIC DRIFT IN PHENOTYPIC EVOLUTION', *Evolution*. Wiley/Blackwell (10.1111), 30(2), pp. 314–334. doi: 10.1111/j.1558-5646.1976.tb00911.x.

Lande and Shannon (1996) 'THE ROLE OF GENETIC VARIATION IN ADAPTATION AND POPULATION PERSISTENCE IN A CHANGING ENVIRONMENT', *Evolution*. Wiley/Blackwell (10.1111), 50(1), pp. 434–437. doi: 10.1111/j.1558-5646.1996.tb04504.x.

van Nes, E. H. and Scheffer, M. (2007) 'Slow recovery from perturbations as a generic indicator of a nearby catastrophic shift.', *The American naturalist*, 169(6), pp. 738–747. doi: 10.1086/516845.

Nolting, B. C. and Abbott, K. C. (2015) 'Balls, cups, and quasi-potentials: quantifying stability in stochastic systems', *Ecology*. Wiley-Blackwell, 97(4), p. 15–1047.1. doi: 10.1890/15-1047.1.

Ozgul, A. *et al.* (2010) 'Coupled dynamics of body mass and population growth in response to environmental change', *Nature*. Nature Publishing Group, 466(7305), pp. 482–485. Available at: http://dx.doi.org/10.1038/nature09210.

Ozgul, A. *et al.* (2014) 'Linking body mass and group dynamics in an obligate cooperative breeder', *Journal of Animal Ecology*. Edited by A. Mysterud. Wiley/Blackwell (10.1111), 83(6), pp. 1357–1366. doi: 10.1111/1365-2656.12239.

Price, T. D., Qvarnström, A. and Irwin, D. E. (2003) 'The role of phenotypic plasticity in driving genetic evolution.', *Proceedings of the Royal Society - Biological sciences*. doi: 10.1098/rspb.2003.2372.

Reed, T. E. *et al.* (2010) 'Phenotypic plasticity and population viability: the importance of environmental predictability.', *Proceedings. Biological sciences / The Royal Society*,

277(1699), pp. 3391–400. doi: 10.1098/rspb.2010.0771.

Reed, T. E., Schindler, D. E. and Waples, R. S. (2011) 'Efectos Interactivos de la Plasticidad Fenot??pica y Evoluc??on sobre la Persistencia Poblacional en un Clima Cambiante', *Conservation Biology*, 25(1), pp. 56–63. doi: 10.1111/j.1523-1739.2010.01552.x.

Robinson, J. D., Wares, J. P. and Drake, J. M. (2013) 'Extinction hazards in experimental Daphnia magna populations: Effects of genotype diversity and environmental variation', *Ecology and Evolution*. doi: 10.1002/ece3.449.

Sanchez, A. and Gore, J. (2013) 'Feedback between Population and Evolutionary Dynamics Determines the Fate of Social Microbial Populations', *PLoS Biology*. Edited by S. P. Ellner, 11(4), p. e1001547. doi: 10.1371/journal.pbio.1001547.

Scheffer *et al.* (2009) 'Early-warning signals for critical transitions.', *Nature*. Nature Publishing Group, 461, pp. 53–59. Available at: http://dx.doi.org/10.1038/nature08227%5Cn%3CGo to ISI%3E://WOS:000269478800026%5Cnhttp://www.nature.com/nature/journal/v461/n7260/pdf/nature08227.pdf.

Scheffer, M. *et al.* (2009) 'Early-warning signals for critical transitions.', *Nature*. Nature Publishing Group, 461(7260), pp. 53–59. doi: 10.1038/nature08227.

Spanbauer, T. L. *et al.* (2016) 'Body size distributions signal a regime shift in a lake ecosystem', *Proceedings of the Royal Society B*, 283, p. 20160249. doi: http://dx.doi.org/10.1098/rspb.2016.0249.

Strogatz, S. H. (1994) 'Nonlinear Dynamics and Chaos', *Book*, pp. 1–505. doi: 9780738204536.

Thomas, C. D. *et al.* (2004) 'Extinction risk from climate change.', *Nature*, 427(6970), pp. 145–8. doi: 10.1038/nature02121.

Villa Martín, P. *et al.* (2015) 'Eluding catastrophic shifts', *Proceedings of the National Academy of Sciences*. doi: 10.1073/pnas.1414708112.

Vuren, D. Van and Armitage, K. B. (1991) 'Duration of snow cover and its influence on life-history variation in yellow-bellied marmots', *Canadian Journal of Zoology*. doi: 10.1139/z91-244.

Wissel, C. (1984) 'A universal law of the characteristic return time near thresholds', *Oecologia*, 65(1), pp. 101–107. doi: 10.1007/BF00384470.

Yoshida, T. *et al.* (2003) 'Rapid evolution drives ecological dynamics in a predator–prey system', *Nature*. doi: 10.1038/nature01767.

Yvonne, W. and Hoffmann, A. A. (2009) 'Demographic factors and genetic variation influence population persistence under environmental change', *Journal of Evolutionary Biology*.

Parameters /variables	*Description*	*Value*
N_t	Abundance of the population at time t	....
$\bar{z}_t$; $\bar{a}_t$	Mean trait value at time t; mean breeding value at time t	....
σ_z^2; σ_a^2	Variance of the mean trait; additive genetic variance or variance of the mean breeding value	[0.05, 0.1, 0.2, 0.3, 0.4,0.5] ; [0.05,0.1, 0.2, 0.3, 0.4,0.5]
b	Strength in phenotypic plasticity	[0.05, 0.1, 0.2,0.3,0.4, 0.5]
R_0	Net reproductive rate	[1.1, 1.2,1.3,1.4, 1.5]
u_t	Environmental cue at time t	$U_t = \begin{cases} 0 & , t < t_{500} \\ 1 - c\frac{t}{500} & , t \geq t_{500} \end{cases}$
θ_t	Optimum phenotype at time t	$\theta_t = BE_t = \begin{cases} 0 & , t < t_{500} \\ B - B\frac{t}{500} & , t \geq t_{500} \end{cases}$ (B = 60)
w_z^2	Width of the Gaussian stabilizing fitness function. A measure of the strength in selection	25
z_i, a_i	Trait value for an individual i ; breeding value for an individual i	....
ϵ	Residual component or unexplained component of a trait z	0
σ_ϵ^2	Variance in that residual component ϵ	0
E_t	External environmental value at time t	....
B	Coefficient that captures the strength in the external environmental change	60
c	Coefficient that controls the rate of change in the environmental cue	1
ξ	Environmental predictability; quantifies how much the external environment is	1

	correlated with the environmental cue	
σ_θ, σ_u	Variance in optimum phenotype, variance in environmental cue	0.8^2, 0.8^2

Table 1: List of parameter values and variables used in the model simulations. The variables are not given any value but factors for which the model simulations are tested are given values.

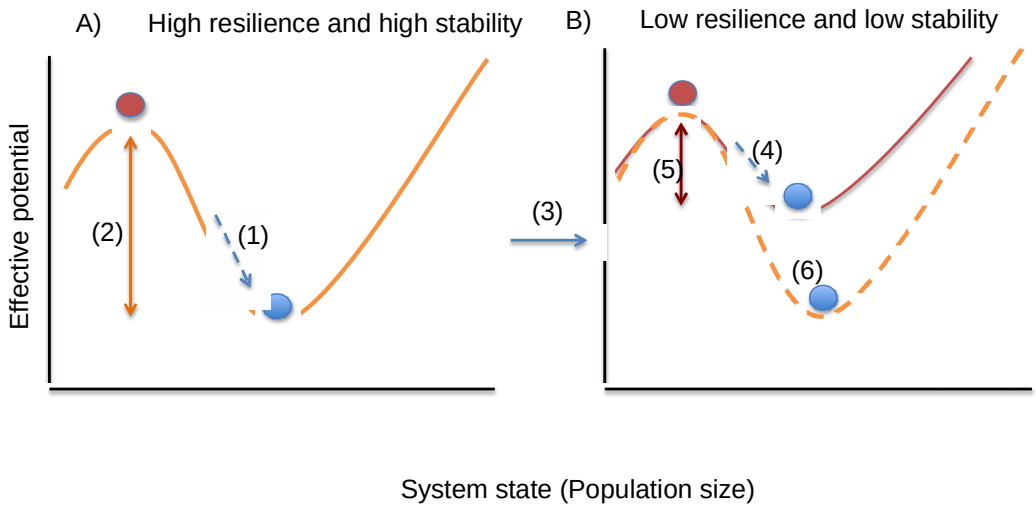

Figure 1. Illustration of the 'ball-in-cup' potential energy curve in relation to stability and resilience of a one-dimensional dynamical system. The stable state of the dynamical system (A) which is an isolated population, can be indicated by the blue ball, and the unstable state (or the tipping point) can be indicated by the red ball in both A and B. (1)- shows that the slope of the potential curve (i.e., stability) is steep and the basin where the ball lies is also deep signifying that both resilience as well as stability is high. This means that the amount of potential energy needed (2) to push the ball from its stable state (blue) to the unstable state (red) (or in other words the reduction in stability) will be large. However, for another isolated population, there might be intrinsic differences in ecological or evolutionary factors controlling the dynamics of that isolated population and this might cause (3) a shift in the 'ball-in-cup' potential energy curve from (6) to (4), for that population. In (4) the slope is now less steep, signifying a reduction in intrinsic

stability. Along with this, there is also a reduction in intrinsic resilience. Now, the amount of potential energy (5) to move the blue ball at (4) to the unstable state for (B) is less. This could reflect in the performances of EWS of population collapse.

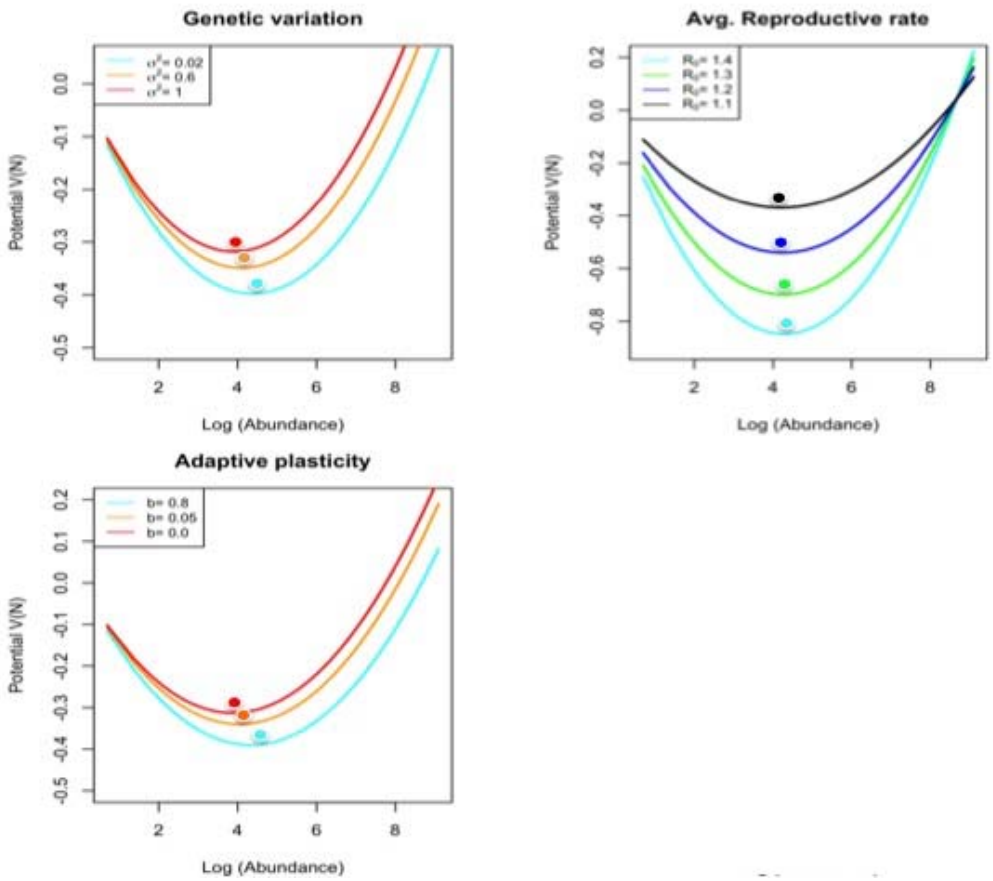

Figure 2. Effective potential plotted as a function of the state variable abundance, N. Note the effective potential is altered by factors like genetic variation, adaptive plasticity and net reproductive rate. The lower the value of the effective potential, more stable the system is.

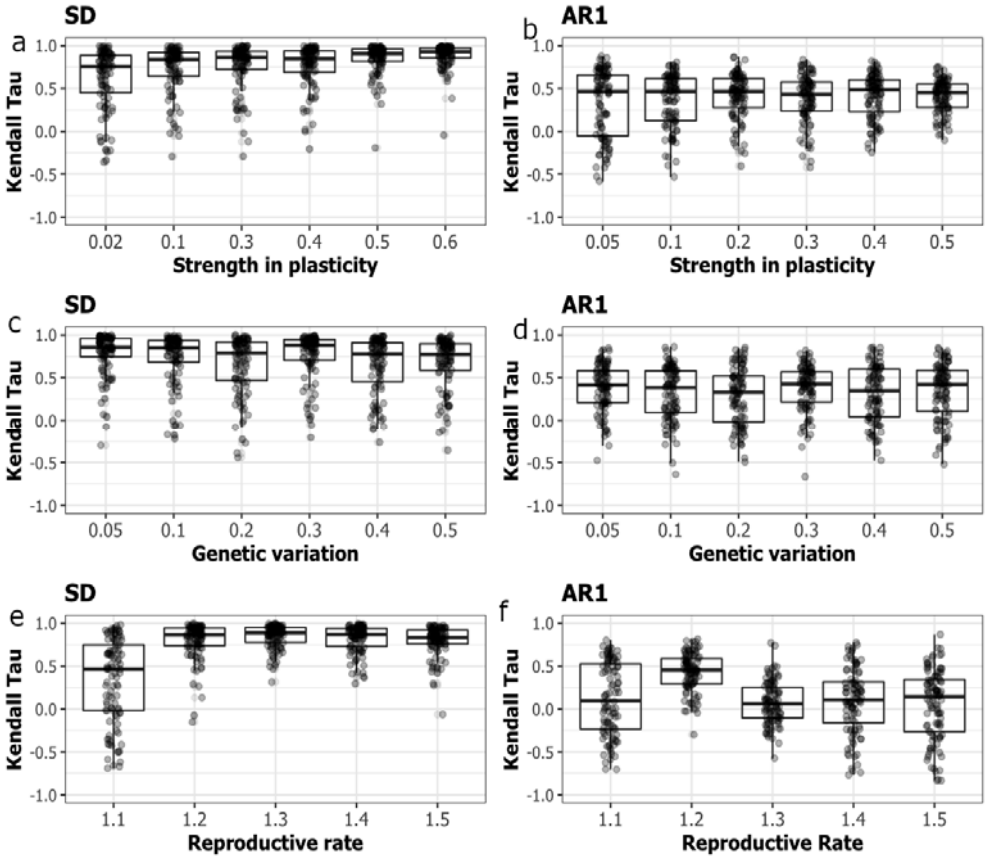

Figure 3. Box plots showing the distribution of Kendall's Tau correlation coefficient (high values around 0.7 are usually considered an EWS) for 100 simulation of population collapse for different levels of adaptive plasticity *b,* genetic variation , reproductive rate R_0. The leading indicators that are shown here are autocorrelation at lag-1 (AR1) and standard deviation (SD). X-axis is the different levels of the above factors.

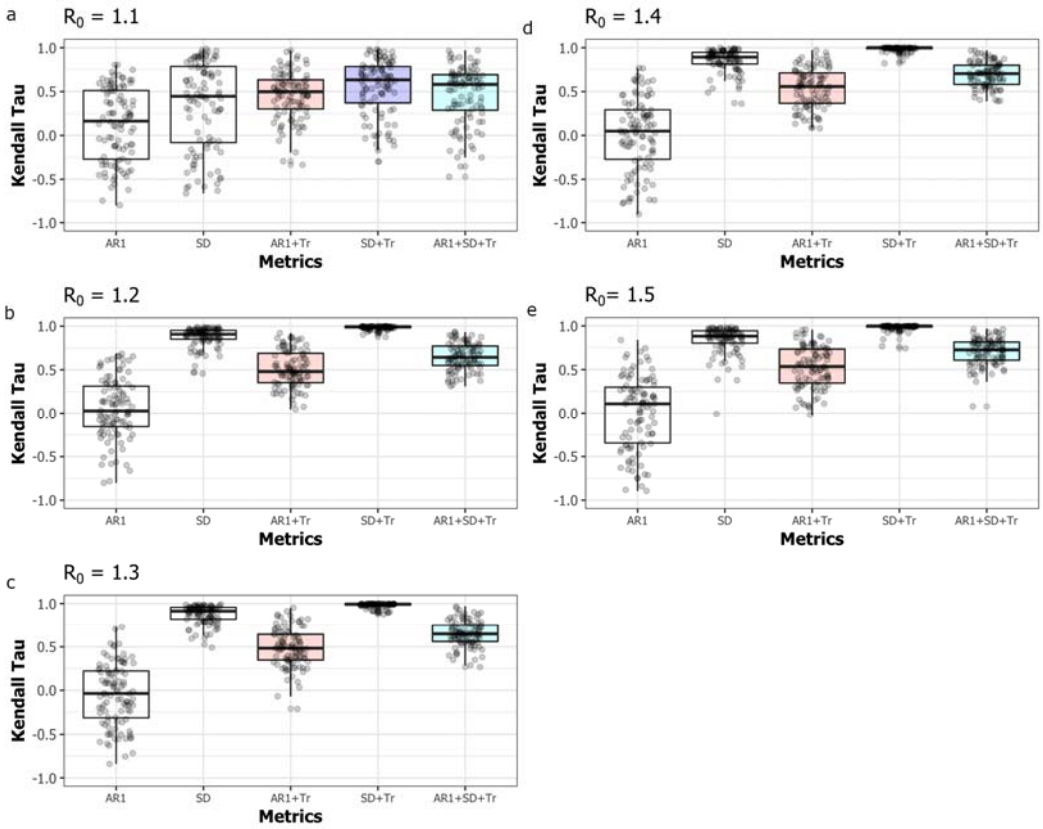

Figure 4. Box plots showing the distribution of Kendall's Tau correlation coefficient for 100 simulation of population collapse for different levels of net reproductive rate R_0. On the X-axis are the different early warning metrics shown : autocorrelation at lag-1 (AR1), standard deviation (SD), (*AR1+Tr*), *(SD+Tr)* ,*(AR1+SD+Tr)*. *Tr* corresponds to the mean value of the phenotypic trait. Colored boxplots denote the trait-based EWS while white boxplots denote abundance-based EWS.

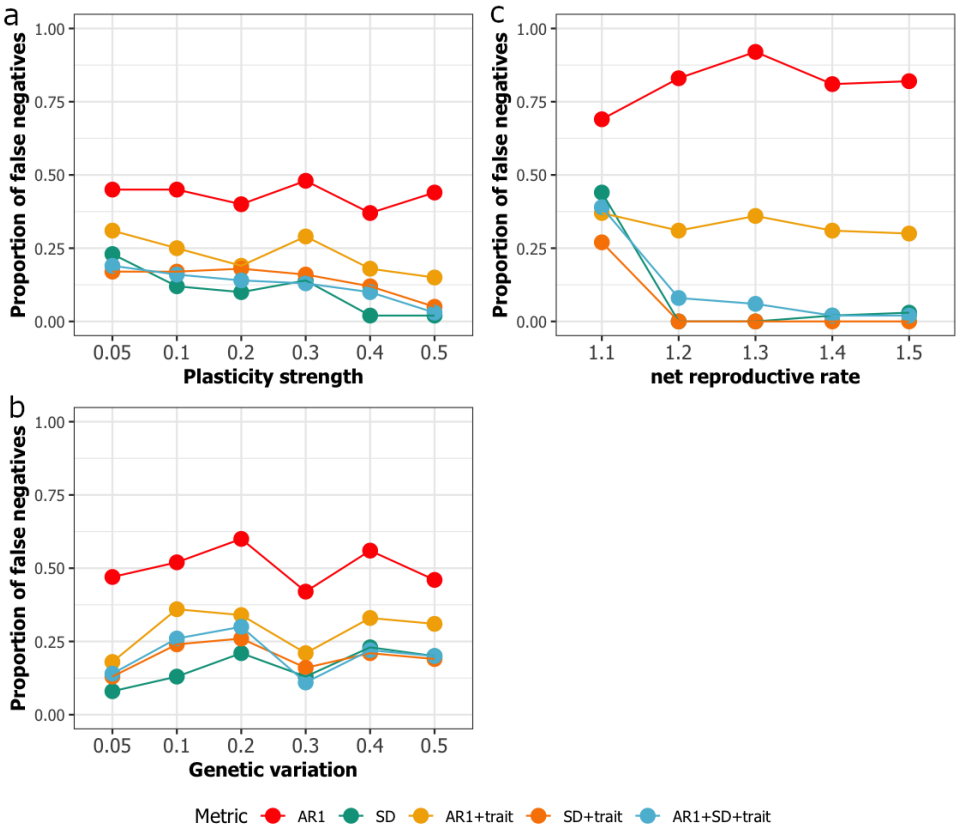

Figure 5. Proportion of false negatives shown here for a threshold of 0.4 (which means Kendall's tau value below 0.4 are considered not an EWS) on the Y-axis for abundance and trait-based EWS metrics for different levels of (a) plasticity strength , (b) genetic variation, (c) net reproductive rate. Note that proportion of false negatives for trait -based EWS particularly *SD+trait* for (c) net-reproductive rate is zero for R_0 values of 1.3, 1.4 and 1.5.